Ka-Band Propagation Modeling for Fixed Satellite Applications

Asoka Dissanayake

COMSAT Laboratories
Clarksburg, Maryland

Abstract- Propagation impairments produced by the troposphere are a limiting factor for the effective use of the 20/30 GHz frequency band. Use of smaller earth terminals, while very attractive for consumer and transportable applications, make it difficult to provide sufficient link margin for propagation related outages. In this context, reliable prediction of propagation impairments for low-availability systems becomes important. This paper addresses the issues related to predicting different types of propagation impairments as well as combining them together to determine the overall impact on satellite links over a wide range of outage probabilities.

I. Introduction

Limitations imposed by the propagation environment makes it difficult to provide Ka-band satellite services at availability levels comparable to those at lower frequency bands. The majority of the planned Ka-band systems are expected to provide services using smaller earth terminals that will neither have sufficient gain nor output power to compensate for more severe propagation effects. Propagation impairments affecting Ka-band satellite links include gaseous absorption, cloud attenuation, rain attenuation, and tropospheric scintillation. Rain attenuation is considered the dominant impairment. A number of prediction models are available for the estimation of individual components. However, methodologies that attempt to combine them in a cohesive manner are not widely available. For small earth terminals, rain effects may only form a relatively small part of the total propagation link margin. It is therefore necessary to identify and predict the overall impact of every significant attenuating effect along any given path. In the absence of detailed knowledge of the occurrence probabilities of different impairments, empirical approaches are taken in estimating their combined effects. Since the propagation impairments originate in the troposphere, the input parameters to the models include meteorological data such as rain rate, cloud cover, temperature, and humidity. To a large extent, the accuracy of the predictions depends on the availability of reliable meteorological data. When designing a satellite network, it is important to have the meteorological data available with a sufficiently high spatial resolution across the satellite coverage area.

Some of the propagation models available for predicting different impairments are discussed in this paper. The discussion is supplemented by results of the recently concluded Ka-band propagation measurement campaign with the Advanced Communication Technology Satellite (ACTS). The measurement program included more than seven sites in North America and the measurement period lasted five years.

II. Propagation Impairments

Propagation factors that affect Ka-band satellite links operating at moderate to high elevation angles include:

- gaseous absorption
- cloud attenuation
- melting layer attenuation
- rain attenuation
- rain and ice depolarization
- tropospheric scintillation

Gaseous absorption, cloud attenuation, melting layer attenuation, and rain attenuation are absorptive effects producing both signal attenuation and a proportionate increase in the thermal noise received at the antenna port. Systems employing orthogonal polarization to implement frequency reuse suffer from interference produced by rain and ice depolarization. Tropospheric scintillation is non-absorptive and produces signal attenuation as well as enhancements. Due consideration must be given to the different impairment factors when evaluating system availability and designing fade mitigation schemes. When modeling propagation impairments cumulative distribution of fades as well as fade dynamics, such as fade rates, fade duration, and frequency scaling behavior of fading mechanisms, must be considered. A brief review of the various propagation factors and associated modeling is presented below.

A. Gaseous Absorption

Compared to other absorptive effects gaseous absorption arising from oxygen and water vapor present in the atmosphere is relatively small. Absorption due to oxygen is nearly constant and that due to water vapor varies slowly with time in response to variations in the water vapor content in the atmosphere. As such, the gaseous absorption increases with the relative humidity as well as the temperature. Gaseous absorption model given in ITU Recommendation 618 [1] can be used to predict statistics of gaseous absorption. Figure 1 shows such a prediction for Washington, DC, at 20 and 30 GHz frequencies; elevation angle is 40°. The distributions were constructed using hourly surface temperature and humidity data. Closeness of the Ka-band down-link frequencies to the water vapor absorption line at 22.2 GHz makes the absorption at 20 GHz to exceed that at 30 GHz. This occurs when the water vapor absorption is significantly larger than the oxygen absorption. It is seen that

for moderate elevation angles the gaseous absorption amounts to less than 1.5 dB under most conditions. The ratio of gaseous absorption between the up- and down-link frequencies is a function of both humidity and temperature and varies approximately between 1.5 for complete dry conditions and 0.8 under high humid conditions.

B. Cloud Attenuation

At Ka-band frequencies clouds containing liquid water can produce both signal attenuation and amplitude scintillation; ice clouds, in general, do not produce these effects. The small size of cloud particles relative to the wavelength makes cloud attenuation essentially a function of cloud temperature and the integrated liquid water content along the propagation path. Depending on the elevation angle and the cloud climatalogy of the earth station site, cloud attenuation levels of as much as 3 dB can be expected at the upper end of the 20/30 GHz frequency band. An example of measured cloud attenuation distribution is shown in Figure 2. ACTS propagation measurements in Clarksburg, MD, at an elevation angle of 39°, were used to extract the cloud attenuation contribution. It is seen that the cloud attenuation at 27.5 GHz can reach values close to 1.5 dB at the given elevation angle. Several models are available for the prediction of cloud attenuation distribution [2-4]. Using the model given in Reference 2, attenuation distributions predicted for the ACTS measurement site are also shown in Fig. 2. It is seen that good agreement between the model prediction and measurements exist. The model is based on the average properties of four types of clouds and long-term cloud cover data obtained by meteorological observation sites. Cloud attenuation (in dBs) is approximately proportional to the square of the frequency. Although reliable information on fading rates associated with clouds is generally lacking, at Ka-band frequencies the fade rates are thought to be relatively small (in the range 0.1 to 1 dB/min).

C. Melting Layer Attenuation

The melting layer is the region around the 0°C isotherm where snow and ice particles from aloft melt to form rain. The presence of a well-defined melting layer or radar bright band is mainly associated with precipitation from stratiform clouds and for low rain rates. The width of the layer is of the order of 500 m. Specific attenuation in the melting layer, however, is expected to be somewhat higher than that in the rain below. Therefore, under light rain and low elevation angle conditions, melting layer attenuation may become a significant factor to the total path attenuation. At higher elevation angles its impact is much reduced; fade levels in the zenith direction amounts to less than 0.5 dB at 30 GHz. References 2 and 5 give methodologies for the prediction of melting layer attenuation.

D. Rain Attenuation

Rain attenuation is the dominant propagation impairment at Ka-band frequencies. Rain attenuation is a function of frequency, elevation angle, polarization angle, rain intensity, raindrop size distribution and raindrop temperature. Fade durations and rates are closely correlated with the rain type; e.g. sratiform rains are conducive to longer fade durations and slower fade rates. Frequency scaling of rain attenuation is largely determined by the raindrop size distribution and the rain temperature.

Several models are available for the prediction of rain attenuation, and the model given in Reference 2 appears to provide good agreement with the Ka-band data collected with the ACTS satellite. The model requires rain rate at the 0.01% probability level as the main input parameter. This can be obtained from measured rain rate distributions or from a rain model such as the Rice-Holmberg model [6], which uses local rain data to derive the rain rate distribution. Since the attenuation model requires only one point in the rain rate distribution, validity of the rain model at this probability level is of particular importance for the attenuation prediction.

Figures 3 and 4 show Ka-band rain attenuation statistics derived from ACTS propagation measurements made in Reston, VA; elevation angle is 39°. The average annual raining time typically is around 5%. The average annual time percentage for which rain attenuation is present along the satellite path is somewhat larger due to the fact that rain attenuation is produced by the rain anywhere along the satellite path and the rain rate distribution pertains only to a point measurement near the earth station antenna.. The distributions shown are for percentage times less than 1%, where other factors such as cloud and melting layer attenuation can be considered absent. The results shown do not include gaseous absorption but includes contributions due to antenna wetting effects. The antenna wetting contribution is a function of the rain intensity, type of antenna used, signal frequency, and the elevation angle. For the measurement site, the antenna wetting contribution at 0.1% is about 2.7 dB at 20.2 GHz and 3.9 dB at 27.5 GHz. Cumulative distributions for five years are shown. It can be seen that a fairly large year-to-year variability exists for lower percentage times. Also shown in the figure is the attenuation distribution predicted with the rain attenuation model given in Reference 2. Measured rain rate distribution was used for the predictions.

Experimental data indicate that rain fade durations are approximately distributed in a log-normal fashion with an average duration close to 5 min. Fade rates are essentially a function of the rain type, and in general, limited to about 1 dB/s.

E. Trpospheric Scintillation

Tropospheric scintillations are amplitude fluctuations produced by refractive inhomogenieties present in the lower

part of the troposphere. Scintillation can occur with or without fading on the path; the former is known as dry scintillation and the latter as wet scintillation since it is accompanied by rain on the path. The magnitude of scintillation increases with the increase of frequency, decrease of elevation angle, and decrease of the antenna diameter. Several empirical models are available for the prediction of scintillation distribution, and the model recommended by the ITU [1] appears to agree with measured results fairly well. The frequency spectrum of scintillation is limited to a maximum frequency of around 2 Hz. Associated fade rates are a function of the peak-to-peak scintillation magnitude and the frequency content. Under severe scintillation conditions fade rates of several dB/s can be expected.

F. Rain and Ice Depolarization

Satellite systems employing frequency re-use by means of orthogonal polarizations may suffer from interference through coupling between wanted and unwanted polarizations. Such coupling arises from antenna imperfections and atmospheric depolarization caused by precipitation particles. Non-spherical particles such as spheroidal raindrops and needle or plate like ice particles can produce coupling between orthogonal polarizations. Rain depolarization is a function of the polarization angle, elevation angle, frequency, and rain attenuation. In the case of linear polarization, depolarization increases with the polarization tilt angle with respect to the local horizontal, and reaches a maximum when the tilt angle is 45°. Depolarization for circularly polarized signals is same as that for a linearly polarized signal having a 45° tilt angle. At Ka-band frequencies rain depolarization becomes significant only at fade levels in excess of about 10 dB. On the other hand ice depolarization can be experienced without significant fading along the link. Rain and ice depolarization may be predicted using empirical techniques such as the one recommended by the ITU [1]. In general, depolarization is of secondary importance compared to rain fading. However, if fade compensation through power control is used, interference caused by depolarization increases proportionately to the amount of power control applied, and due care must be taken to avoid excessive interference.

III Combined Effect of Propagation Impairments

The preceding section outlined the individual propagation impairments affecting Ka-band satellite links. All the propagation impairments discussed so far originate in the lower troposphere and their respective sources are highly interdependent. Some examples are: cumulus clouds can produce both attenuation and scintillation; the melting layer is associated with low-intensity rain; gaseous absorption increases during rain due to the increased water vapor content in the atmosphere. Simultaneous occurrence of different impairments are illustrated in Figure 5, where spectral decomposition is used to identify the propagation factors. A fade event recorded at Clarksburg, MD, using the ACTS beacon signals is shown in Fig. 5a. Fig. 5b shows the ratio of the logarithm of the spectral components of the event. As shown in the figure, different propagation factors can be identified through the spectral ratio. Lower frequency components of the ratio are identified with gaseous absorption, mid frequencies are associated with clouds and rain, and higher values are produced by scintillation activity.

Frequency domain separation of propagation factors can be gainfully employed when implementing fade mitigation techniques. However, a procedure for combining the different impairments to produce an overall cumulative fade distribution is not directly evident from this type of analysis. This is compounded by the fact that most impairment prediction models are semi-empirical in nature due to an incomplete understanding of the physical mechanisms as well as the lack of an adequate characterization of the various sources producing the impairments. Methodologies available for combining impairments generally limit themselves to combining only the absorptive and non-absorptive components. A comprehensive combining methodology is given in Reference 2. Use of this combining approach is illustrated in Figure 6 where the distribution of signal attenuation observed at 20.2 and 27.5 GHz at Clarksburg, MD are shown. Total path attenuation that includes gaseous absorption and other clear-air effects are included in the distributions. The distributions are shown for percentage times between 10% and 1% where several propagation factors are expected to contribute toward the total attenuation. The annual raining time for the measurement site is around 2%. It is seen that the model can replicate the measured results reasonably well.

IV Implications on Satellite System Design

Satellite systems are designed to provide a predetermined level of service availability and hence must take account of the variation in path attenuation and associated outage times within the satellite coverage area. Sizing of antennas and power amplifiers, selection of fade mitigation techniques, and allocation of fade margins are some of the design considerations which address propagation outages. Considerable variation of attenuation across the satellite coverage area is fairly common, and the system design can be optimized by analyzing such variations. As an example, additional space segment resources can be allocated to areas with higher propagation outages in comparison to areas with lower outages. In order to investigate the variability of attenuation over a given satellite coverage area, calculations must be made using a dense grid of points with representative input data for the propagation models. The grid density must be such that it will account for small-scale variations in climatology brought about by terrain features. A grid spacing of the order of few tens of kilometers is required to capture

such variability. It is not always possible to obtain climatic data with this level of spatial resolution. At least in some parts of the world, e.g. USA, Europe, and Japan, data with a resolution approaching the required value are available. To determine the variability of attenuation across a typical satellite coverage area, contour plots of attenuation exceeded for a specified availability can be generated. An example of such a contour plot at 20 GHz is shown in Figure 7, where the system availability is specified at 99.9%. The calculations were performed using the model in Reference 2 for a satellite located at 100°W. For the selected frequency and availability, rain is considered the dominant contributing factor to the overall attenuation. The Rice-Holmberg rain model with input parameter grid resolution of 0.25°x0.25° in longitude and latitude was used for the calculations. It is seen that the attenuation variation at the selected availability is fairly large, ranging from 4 dB to as much as 16 dB. Some of the variation can be reduced by using static compensation techniques such as providing additional satellite EIRP toward the areas experiencing higher fades, while reducing the EIRP for areas with shallow fading. Dynamic fade compensation techniques are also applicable, and these include data rate reduction and adaptive power control. A similar situation is present for the up-link and countering of fading in this case may be accomplished by increasing the satellite antenna gain towards the affected area and using up-link power control in earth terminals.

V. SUMMARY

Propagation modeling applicable for Ka-band satellite system design was outlined by identifying individual impairments and a way to obtain their combined effect. Results from the recent Ka-band propagation measurements conducted with the ACTS satellite were cited to validate the modeling approaches presented. Variability of propagation effects across a typical satellite coverage area was illustrated to highlight the system optimization that can potentially be carried out with climatic data with high spatial resolution. At Ka-band, significant variability in attenuation exists over the satellite coverage area, and a number of methods are available to redistribute space segment resources to even out the variability of propagation effects.

VI. REFERENCES

[1] ITU Recommendation ITU RPN.618, 1996

[2] A. W. Dissanayake, J. E. Allnutt, F. Haidara, "A Prediction Model that Combines Rain Attenuation and Other Propagation Impairments Along Earth-Satellite Paths," *IEEE Trans*. AP 45, pp 1546-1558, October, 1997

[3] E. Salonen and S. Uppala, "New prediction method of cloud attenuation," *Electronics Letters*, Vol 27, pp.1106-1108, 1991

[4] D. S. Slobin, "Microwave noise temperature and attenuation of clouds: Statistics of these effects at various sites in the United States, Alaska, and Hawaii," *Radio Science*, Vol. 17, pp. 1443-1454, 1982

[5] W. Zhang, et. al., "Prediction of radio wave attenuation due to melting layer of precipitation," *IEEE Trans.* AP.-42, pp. 492-500, 1994

[6] P. L. Rice, N. R. Holmberg, "Cumulative time statistics of surface point rainfall rates," *IEEE Trans*. Com-21, pp 1131-1136, 1973

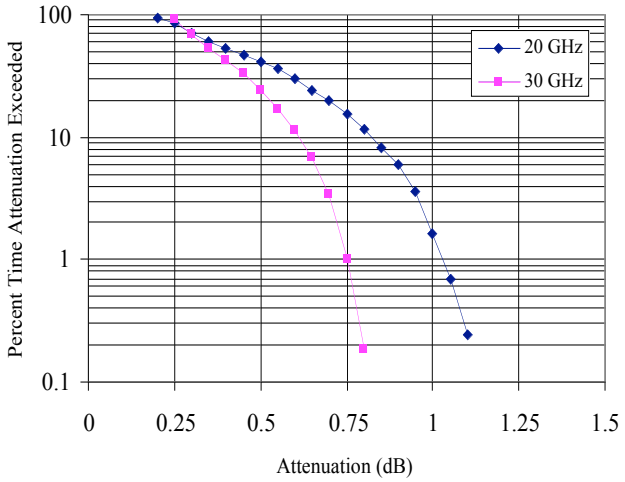

Figure 1 Gaseous absorption distributions at 20 and 30 GHz; Washington, DC; Elevation angle is 40°

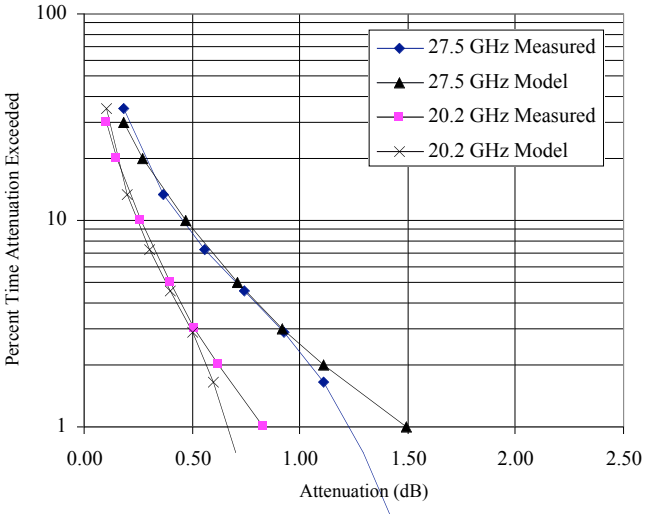

Figure 2 Cloud attenuation distributions at 20.2 and 27.5 GHz; Clarksburg, MD; Elevation angle is 39°

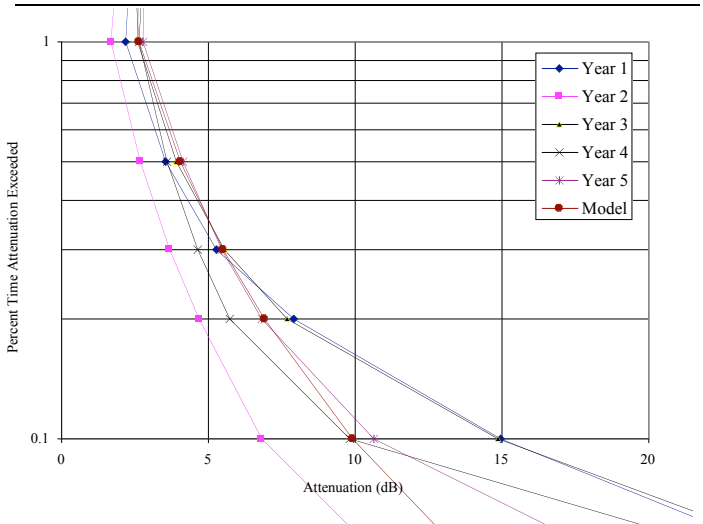

Figure 3. Rain attenuation distribution at 20.2 GHz; Reston, VA; Elevation angle is 39°

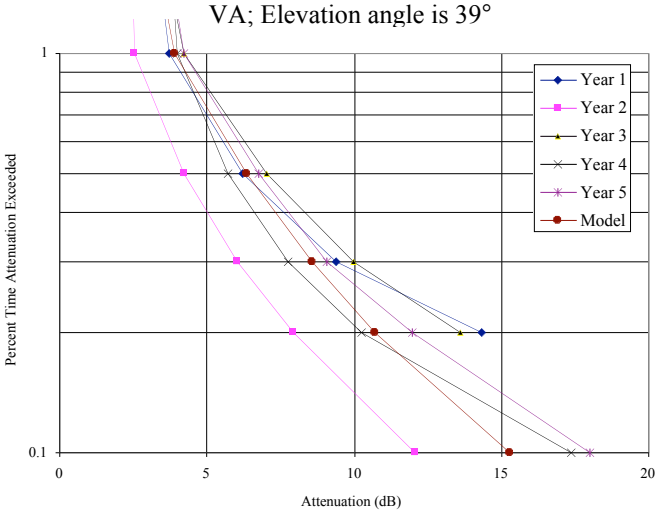

Figure 4. Rain attenuation distributions at 27.5 GHz; Reston, VA; Elevation angle is 39°

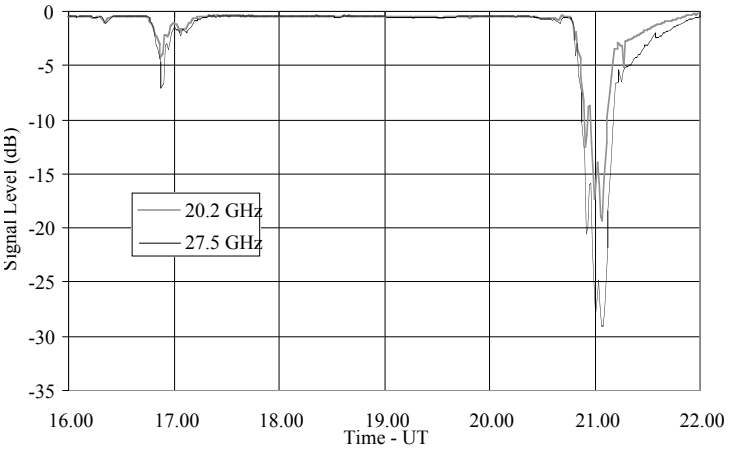

Figure 5a. Rain event observed at Clarksburg, MD

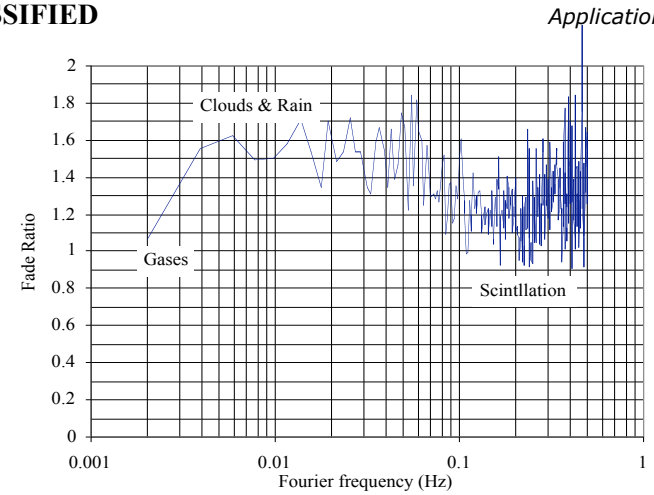

Figure 5b Ratio of spectral components corresponding to Fig 5a

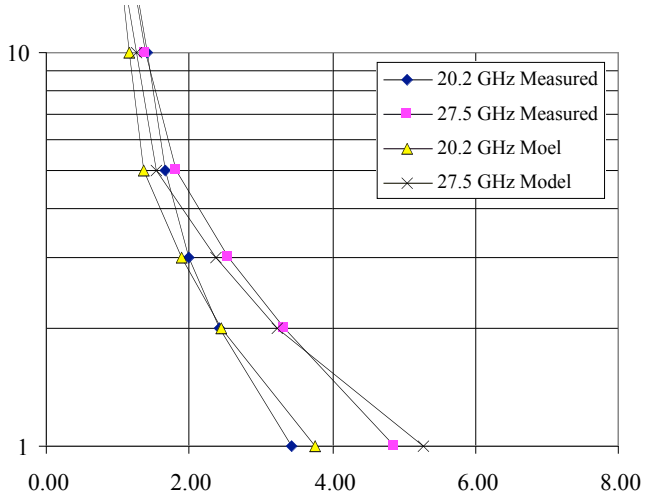

Figure 6. Attenuation distributions at 20.2 and 27.5 GHz; Clarksburg, MD; Elevation angle is 39°

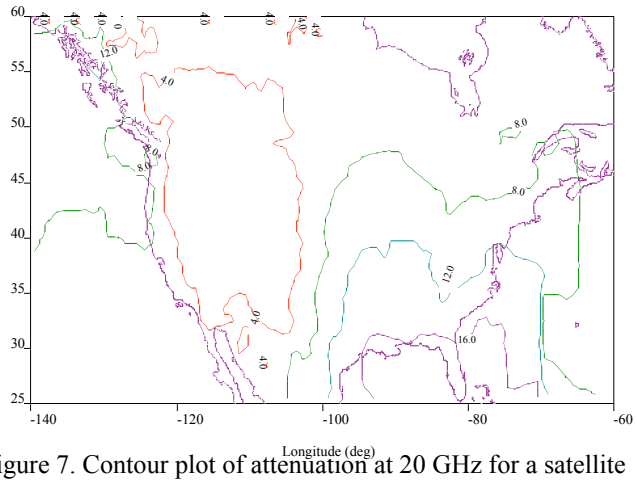

Figure 7. Contour plot of attenuation at 20 GHz for a satellite locatted at 100°W.